Fermilab-Pub-04/08-010-E

Simultaneous measurement of the ratio $\mathcal{B}(t \to Wb)/\mathcal{B}(t \to Wq)$ and the top quark pair production cross section with the D0 detector at $\sqrt{s} = 1.96$ TeV

V.M. Abazov[36], B. Abbott[76], M. Abolins[66], B.S. Acharya[29], M. Adams[52], T. Adams[50], E. Aguilo[6], S.H. Ahn[31], M. Ahsan[60], G.D. Alexeev[36], G. Alkhazov[40], A. Alton[65,a], G. Alverson[64], G.A. Alves[2], M. Anastasoaie[35], L.S. Ancu[35], T. Andeen[54], S. Anderson[46], B. Andrieu[17], M.S. Anzelc[54], Y. Arnoud[14], M. Arov[61], M. Arthaud[18], A. Askew[50], B. Åsman[41], A.C.S. Assis Jesus[3], O. Atramentov[50], C. Autermann[21], C. Avila[8], C. Ay[24], F. Badaud[13], A. Baden[62], L. Bagby[53], B. Baldin[51], D.V. Bandurin[60], S. Banerjee[29], P. Banerjee[29], E. Barberis[64], A.-F. Barfuss[15], P. Bargassa[81], P. Baringer[59], J. Barreto[2], J.F. Bartlett[51], U. Bassler[18], D. Bauer[44], S. Beale[6], A. Bean[59], M. Begalli[3], M. Begel[72], C. Belanger-Champagne[41], L. Bellantoni[51], A. Bellavance[51], J.A. Benitez[66], S.B. Beri[27], G. Bernardi[17], R. Bernhard[23], I. Bertram[43], M. Besançon[18], R. Beuselinck[44], V.A. Bezzubov[39], P.C. Bhat[51], V. Bhatnagar[27], C. Biscarat[20], G. Blazey[53], F. Blekman[44], S. Blessing[50], D. Bloch[19], K. Bloom[68], A. Boehnlein[51], D. Boline[63], T.A. Bolton[60], G. Borissov[43], T. Bose[78], A. Brandt[79], R. Brock[66], G. Brooijmans[71], A. Bross[51], D. Brown[82], N.J. Buchanan[50], D. Buchholz[54], M. Buehler[82], V. Buescher[22], V. Bunichev[38], S. Burdin[43,b], S. Burke[46], T.H. Burnett[83], C.P. Buszello[44], J.M. Butler[63], P. Calfayan[25], S. Calvet[16], J. Cammin[72], W. Carvalho[3], B.C.K. Casey[51], N.M. Cason[56], H. Castilla-Valdez[33], S. Chakrabarti[18], D. Chakraborty[53], K.M. Chan[56], K. Chan[6], A. Chandra[49], F. Charles[19,‡], E. Cheu[46], F. Chevallier[14], D.K. Cho[63], S. Choi[32], B. Choudhary[28], L. Christofek[78], T. Christoudias[44,†], S. Cihangir[51], D. Claes[68], Y. Coadou[6], M. Cooke[81], W.E. Cooper[51], M. Corcoran[81], F. Couderc[18], M.-C. Cousinou[15], S. Crépé-Renaudin[14], D. Cutts[78], M. Ćwiok[30], H. da Motta[2], A. Das[46], G. Davies[44], K. De[79], S.J. de Jong[35], E. De La Cruz-Burelo[65], C. De Oliveira Martins[3], J.D. Degenhardt[65], F. Déliot[18], M. Demarteau[51], R. Demina[72], D. Denisov[51], S.P. Denisov[39], S. Desai[51], H.T. Diehl[51], M. Diesburg[51], A. Dominguez[68], H. Dong[73], L.V. Dudko[38], L. Duflot[16], S.R. Dugad[29], D. Duggan[50], A. Duperrin[15], J. Dyer[66], A. Dyshkant[53], M. Eads[68], D. Edmunds[66], J. Ellison[49], V.D. Elvira[51], Y. Enari[78], S. Eno[62], P. Ermolov[38], H. Evans[55], A. Evdokimov[74], V.N. Evdokimov[39], A.V. Ferapontov[60], T. Ferbel[72], F. Fiedler[24], F. Filthaut[35], W. Fisher[51], H.E. Fisk[51], M. Ford[45], M. Fortner[53], H. Fox[23], S. Fu[51], S. Fuess[51], T. Gadfort[71], C.F. Galea[35], E. Gallas[51], E. Galyaev[56], C. Garcia[72], A. Garcia-Bellido[83], V. Gavrilov[37], P. Gay[13], W. Geist[19], D. Gelé[19], C.E. Gerber[52], Y. Gershtein[50], D. Gillberg[6], G. Ginther[72], N. Gollub[41], B. Gómez[8], A. Goussiou[56], P.D. Grannis[73], H. Greenlee[51], Z.D. Greenwood[61], E.M. Gregores[4], G. Grenier[20], Ph. Gris[13], J.-F. Grivaz[16], A. Grohsjean[25], S. Grünendahl[51], M.W. Grünewald[30], J. Guo[73], F. Guo[73], P. Gutierrez[76], G. Gutierrez[51], A. Haas[71], N.J. Hadley[62], P. Haefner[25], S. Hagopian[50], J. Haley[69], I. Hall[66], R.E. Hall[48], L. Han[7], P. Hansson[41], K. Harder[45], A. Harel[72], R. Harrington[64], J.M. Hauptman[58], R. Hauser[66], J. Hays[44], T. Hebbeker[21], D. Hedin[53], J.G. Hegeman[34], J.M. Heinmiller[52], A.P. Heinson[49], U. Heintz[63], C. Hensel[59], K. Herner[73], G. Hesketh[64], M.D. Hildreth[56], R. Hirosky[82], J.D. Hobbs[73], B. Hoeneisen[12], H. Hoeth[26], M. Hohlfeld[22], S.J. Hong[31], S. Hossain[76], P. Houben[34], Y. Hu[73], Z. Hubacek[10], V. Hynek[9], I. Iashvili[70], R. Illingworth[51], A.S. Ito[51], S. Jabeen[63], M. Jaffré[16], S. Jain[76], K. Jakobs[23], C. Jarvis[62], R. Jesik[44], K. Johns[46], C. Johnson[71], M. Johnson[51], A. Jonckheere[51], P. Jonsson[44], A. Juste[51], E. Kajfasz[15], A.M. Kalinin[36], J.R. Kalk[66], J.M. Kalk[61], S. Kappler[21], D. Karmanov[38], P.A. Kasper[51], I. Katsanos[71], D. Kau[50], R. Kaur[27], V. Kaushik[79], R. Kehoe[80], S. Kermiche[15], N. Khalatyan[51], A. Khanov[77], A. Kharchilava[70], Y.M. Kharzheev[36], D. Khatidze[71], T.J. Kim[31], M.H. Kirby[54], M. Kirsch[21], B. Klima[51], J.M. Kohli[27], J.-P. Konrath[23], V.M. Korablev[39], A.V. Kozelov[39], D. Krop[55], T. Kuhl[24], A. Kumar[70], S. Kunori[62], A. Kupco[11], T. Kurča[20], J. Kvita[9,†], F. Lacroix[13], D. Lam[56], S. Lammers[71], G. Landsberg[78], P. Lebrun[20], W.M. Lee[51], A. Leflat[38], F. Lehner[42], J. Lellouch[17], J. Leveque[46], J. Li[79], Q.Z. Li[51], L. Li[49], S.M. Lietti[5], J.G.R. Lima[53], D. Lincoln[51], J. Linnemann[66], V.V. Lipaev[39], R. Lipton[51], Y. Liu[7,†], Z. Liu[6], A. Lobodenko[40], M. Lokajicek[11], P. Love[43], H.J. Lubatti[83], R. Luna[3], A.L. Lyon[51], A.K.A. Maciel[2], D. Mackin[81], R.J. Madaras[47], P. Mättig[26], C. Magass[21], A. Magerkurth[65], P.K. Mal[56], H.B. Malbouisson[3], S. Malik[68], V.L. Malyshev[36], H.S. Mao[51], Y. Maravin[60], B. Martin[14], R. McCarthy[73], A. Melnitchouk[67], L. Mendoza[8], P.G. Mercadante[5], M. Merkin[38], K.W. Merritt[51], J. Meyer[22,d], A. Meyer[21], T. Millet[20], J. Mitrevski[71], J. Molina[3], R.K. Mommsen[45], N.K. Mondal[29], R.W. Moore[6], T. Moulik[59], G.S. Muanza[20], M. Mulders[51], M. Mulhearn[71], O. Mundal[22], L. Mundim[3], E. Nagy[15], M. Naimuddin[51], M. Narain[78], N.A. Naumann[35], H.A. Neal[65], J.P. Negret[8], P. Neustroev[40], H. Nilsen[23], H. Nogima[3], S.F. Novaes[5], T. Nunnemann[25], V. O'Dell[51], D.C. O'Neil[6], G. Obrant[40], C. Ochando[16], D. Onoprienko[60], N. Oshima[51], J. Osta[56], R. Otec[10], G.J. Otero y Garzón[51], M. Owen[45],

P. Padley[81], M. Pangilinan[78], N. Parashar[57], S.-J. Park[72], S.K. Park[31], J. Parsons[71], R. Partridge[78], N. Parua[55], A. Patwa[74], G. Pawloski[81], B. Penning[23], M. Perfilov[38], K. Peters[45], Y. Peters[26], P. Pétroff[16], M. Petteni[44], R. Piegaia[1], J. Piper[66], M.-A. Pleier[22], P.L.M. Podesta-Lerma[33,c], V.M. Podstavkov[51], Y. Pogorelov[56], M.-E. Pol[2], P. Polozov[37], B.G. Pope[66], A.V. Popov[39], C. Potter[6], W.L. Prado da Silva[3], H.B. Prosper[50], S. Protopopescu[74], J. Qian[65], A. Quadt[22,d], B. Quinn[67], A. Rakitine[43], M.S. Rangel[2], K. Ranjan[28], P.N. Ratoff[43], P. Renkel[80], S. Reucroft[64], P. Rich[45], J. Rieger[55], M. Rijssenbeek[73], I. Ripp-Baudot[19], F. Rizatdinova[77], S. Robinson[44], R.F. Rodrigues[3], M. Rominsky[76], C. Royon[18], P. Rubinov[51], R. Ruchti[56], G. Safronov[37], G. Sajot[14], A. Sánchez-Hernández[33], M.P. Sanders[17], A. Santoro[3], G. Savage[51], L. Sawyer[61], T. Scanlon[44], D. Schaile[25], R.D. Schamberger[73], Y. Scheglov[40], H. Schellman[54], T. Schliephake[26], C. Schwanenberger[45], A. Schwartzman[69], R. Schwienhorst[66], J. Sekaric[50], H. Severini[76], E. Shabalina[52], M. Shamim[60], V. Shary[18], A.A. Shchukin[39], R.K. Shivpuri[28], V. Siccardi[19], V. Simak[10], V. Sirotenko[51], P. Skubic[76], P. Slattery[72], D. Smirnov[56], J. Snow[75], G.R. Snow[68], S. Snyder[74], S. Söldner-Rembold[45], L. Sonnenschein[17], A. Sopczak[43], M. Sosebee[79], K. Soustruznik[9], B. Spurlock[79], J. Stark[14], J. Steele[61], V. Stolin[37], D.A. Stoyanova[39], J. Strandberg[65], S. Strandberg[41], M.A. Strang[70], M. Strauss[76], E. Strauss[73], R. Ströhmer[25], D. Strom[54], L. Stutte[51], S. Sumowidagdo[50], P. Svoisky[56], A. Sznajder[3], M. Talby[15], P. Tamburello[46], A. Tanasijczuk[1], W. Taylor[6], J. Temple[46], B. Tiller[25], F. Tissandier[13], M. Titov[18], V.V. Tokmenin[36], T. Toole[62], I. Torchiani[23], T. Trefzger[24], D. Tsybychev[73], B. Tuchming[18], C. Tully[69], P.M. Tuts[71], R. Unalan[66], S. Uvarov[40], L. Uvarov[40], S. Uzunyan[53], B. Vachon[6], P.J. van den Berg[34], R. Van Kooten[55], W.M. van Leeuwen[34], N. Varelas[52], E.W. Varnes[46], I.A. Vasilyev[39], M. Vaupel[26], P. Verdier[20], L.S. Vertogradov[36], M. Verzocchi[51], F. Villeneuve-Seguier[44], P. Vint[44], P. Vokac[10], E. Von Toerne[60], M. Voutilainen[68,e], R. Wagner[69], H.D. Wahl[50], L. Wang[62], M.H.L.S Wang[51], J. Warchol[56], G. Watts[83], M. Wayne[56], M. Weber[51], G. Weber[24], L. Welty-Rieger[55], A. Wenger[42], N. Wermes[22], M. Wetstein[62], A. White[79], D. Wicke[26], G.W. Wilson[59], S.J. Wimpenny[49], M. Wobisch[61], D.R. Wood[64], T.R. Wyatt[45], Y. Xie[78], S. Yacoob[54], R. Yamada[51], M. Yan[62], T. Yasuda[51], Y.A. Yatsunenko[36], K. Yip[74], H.D. Yoo[78], S.W. Youn[54], J. Yu[79], A. Zatserklyaniy[53], C. Zeitnitz[26], T. Zhao[83], B. Zhou[65], J. Zhu[73], M. Zielinski[72], D. Zieminska[55], A. Zieminski[55,‡], L. Zivkovic[71], V. Zutshi[53], and E.G. Zverev[38]

(The DØ Collaboration)

[1]*Universidad de Buenos Aires, Buenos Aires, Argentina*
[2]*LAFEX, Centro Brasileiro de Pesquisas Físicas, Rio de Janeiro, Brazil*
[3]*Universidade do Estado do Rio de Janeiro, Rio de Janeiro, Brazil*
[4]*Universidade Federal do ABC, Santo André, Brazil*
[5]*Instituto de Física Teórica, Universidade Estadual Paulista, São Paulo, Brazil*
[6]*University of Alberta, Edmonton, Alberta, Canada, Simon Fraser University, Burnaby, British Columbia, Canada, York University, Toronto, Ontario, Canada, and McGill University, Montreal, Quebec, Canada*
[7]*University of Science and Technology of China, Hefei, People's Republic of China*
[8]*Universidad de los Andes, Bogotá, Colombia*
[9]*Center for Particle Physics, Charles University, Prague, Czech Republic*
[10]*Czech Technical University, Prague, Czech Republic*
[11]*Center for Particle Physics, Institute of Physics, Academy of Sciences of the Czech Republic, Prague, Czech Republic*
[12]*Universidad San Francisco de Quito, Quito, Ecuador*
[13]*LPC, Univ Blaise Pascal, CNRS/IN2P3, Clermont, France*
[14]*LPSC, Université Joseph Fourier Grenoble 1, CNRS/IN2P3, Institut National Polytechnique de Grenoble, France*
[15]*CPPM, IN2P3/CNRS, Université de la Méditerranée, Marseille, France*
[16]*LAL, Univ Paris-Sud, IN2P3/CNRS, Orsay, France*
[17]*LPNHE, IN2P3/CNRS, Universités Paris VI and VII, Paris, France*
[18]*DAPNIA/Service de Physique des Particules, CEA, Saclay, France*
[19]*IPHC, Université Louis Pasteur et Université de Haute Alsace, CNRS/IN2P3, Strasbourg, France*
[20]*IPNL, Université Lyon 1, CNRS/IN2P3, Villeurbanne, France and Université de Lyon, Lyon, France*
[21]*III. Physikalisches Institut A, RWTH Aachen, Aachen, Germany*
[22]*Physikalisches Institut, Universität Bonn, Bonn, Germany*
[23]*Physikalisches Institut, Universität Freiburg, Freiburg, Germany*
[24]*Institut für Physik, Universität Mainz, Mainz, Germany*
[25]*Ludwig-Maximilians-Universität München, München, Germany*

[26]*Fachbereich Physik, University of Wuppertal, Wuppertal, Germany*
[27]*Panjab University, Chandigarh, India*
[28]*Delhi University, Delhi, India*
[29]*Tata Institute of Fundamental Research, Mumbai, India*
[30]*University College Dublin, Dublin, Ireland*
[31]*Korea Detector Laboratory, Korea University, Seoul, Korea*
[32]*SungKyunKwan University, Suwon, Korea*
[33]*CINVESTAV, Mexico City, Mexico*
[34]*FOM-Institute NIKHEF and University of Amsterdam/NIKHEF, Amsterdam, The Netherlands*
[35]*Radboud University Nijmegen/NIKHEF, Nijmegen, The Netherlands*
[36]*Joint Institute for Nuclear Research, Dubna, Russia*
[37]*Institute for Theoretical and Experimental Physics, Moscow, Russia*
[38]*Moscow State University, Moscow, Russia*
[39]*Institute for High Energy Physics, Protvino, Russia*
[40]*Petersburg Nuclear Physics Institute, St. Petersburg, Russia*
[41]*Lund University, Lund, Sweden, Royal Institute of Technology and Stockholm University, Stockholm, Sweden, and Uppsala University, Uppsala, Sweden*
[42]*Physik Institut der Universität Zürich, Zürich, Switzerland*
[43]*Lancaster University, Lancaster, United Kingdom*
[44]*Imperial College, London, United Kingdom*
[45]*University of Manchester, Manchester, United Kingdom*
[46]*University of Arizona, Tucson, Arizona 85721, USA*
[47]*Lawrence Berkeley National Laboratory and University of California, Berkeley, California 94720, USA*
[48]*California State University, Fresno, California 93740, USA*
[49]*University of California, Riverside, California 92521, USA*
[50]*Florida State University, Tallahassee, Florida 32306, USA*
[51]*Fermi National Accelerator Laboratory, Batavia, Illinois 60510, USA*
[52]*University of Illinois at Chicago, Chicago, Illinois 60607, USA*
[53]*Northern Illinois University, DeKalb, Illinois 60115, USA*
[54]*Northwestern University, Evanston, Illinois 60208, USA*
[55]*Indiana University, Bloomington, Indiana 47405, USA*
[56]*University of Notre Dame, Notre Dame, Indiana 46556, USA*
[57]*Purdue University Calumet, Hammond, Indiana 46323, USA*
[58]*Iowa State University, Ames, Iowa 50011, USA*
[59]*University of Kansas, Lawrence, Kansas 66045, USA*
[60]*Kansas State University, Manhattan, Kansas 66506, USA*
[61]*Louisiana Tech University, Ruston, Louisiana 71272, USA*
[62]*University of Maryland, College Park, Maryland 20742, USA*
[63]*Boston University, Boston, Massachusetts 02215, USA*
[64]*Northeastern University, Boston, Massachusetts 02115, USA*
[65]*University of Michigan, Ann Arbor, Michigan 48109, USA*
[66]*Michigan State University, East Lansing, Michigan 48824, USA*
[67]*University of Mississippi, University, Mississippi 38677, USA*
[68]*University of Nebraska, Lincoln, Nebraska 68588, USA*
[69]*Princeton University, Princeton, New Jersey 08544, USA*
[70]*State University of New York, Buffalo, New York 14260, USA*
[71]*Columbia University, New York, New York 10027, USA*
[72]*University of Rochester, Rochester, New York 14627, USA*
[73]*State University of New York, Stony Brook, New York 11794, USA*
[74]*Brookhaven National Laboratory, Upton, New York 11973, USA*
[75]*Langston University, Langston, Oklahoma 73050, USA*
[76]*University of Oklahoma, Norman, Oklahoma 73019, USA*
[77]*Oklahoma State University, Stillwater, Oklahoma 74078, USA*
[78]*Brown University, Providence, Rhode Island 02912, USA*
[79]*University of Texas, Arlington, Texas 76019, USA*
[80]*Southern Methodist University, Dallas, Texas 75275, USA*
[81]*Rice University, Houston, Texas 77005, USA*
[82]*University of Virginia, Charlottesville, Virginia 22901, USA and*
[83]*University of Washington, Seattle, Washington 98195, USA*

(Dated: January 8, 2008)

We present the first simultaneous measurement of the ratio of branching fractions, $R = \mathcal{B}(t \to Wb)/\mathcal{B}(t \to Wq)$, with q being a d, s, or b quark, and the top quark pair production cross section $\sigma_{t\bar{t}}$ in the lepton plus jets channel using 0.9 fb^{-1} of $p\bar{p}$ collision data at $\sqrt{s} = 1.96$ TeV collected with

the D0 detector. We extract R and $\sigma_{t\bar{t}}$ by analyzing samples of events with 0, 1 and ≥ 2 identified b jets. We measure $R = 0.97^{+0.09}_{-0.08}$ (stat+syst) and $\sigma_{t\bar{t}} = 8.18^{+0.90}_{-0.84}$ (stat+syst) $\pm$ 0.50 (lumi) pb, in agreement with the standard model prediction.

PACS numbers: 13.85.Lg, 13.85.Qk, 14.65.Ha

Within the standard model (SM) the top quark decays to a W boson and a down-type quark q ($q = d, s, b$) with a rate proportional to the squared Cabibbo-Kobayashi-Maskawa (CKM) matrix element, $|V_{tq}|^2$ [1]. Under the assumption of three fermion families and a unitary 3×3 CKM matrix, the $|V_{tq}|$ elements are severely constrained: $|V_{td}| = (7.4 \pm 0.8) \cdot 10^{-3}$, $|V_{ts}| = (40.6 \pm 2.7) \cdot 10^{-3}$ and $|V_{tb}| = 0.999100^{+0.000034}_{-0.000004}$ [2]. However, in several extensions of the SM the 3×3 CKM submatrix would not appear unitary and $|V_{tq}|$ elements can significantly deviate from their SM values. This would affect the rate for single top quarks production via the electroweak interaction [3] and the ratio R of the top quark branching fractions, which can be expressed in terms of the CKM matrix elements as

$$R = \frac{\mathcal{B}(t \to Wb)}{\mathcal{B}(t \to Wq)} = \frac{\mid V_{tb} \mid^2}{\mid V_{tb} \mid^2 + \mid V_{ts} \mid^2 + \mid V_{td} \mid^2} .$$

A precise measurement of R is therefore a necessary ingredient for performing direct measurements, free of assumptions about the number of quark families or the unitarity of the CKM matrix, of the $|V_{tq}|$ elements via the combination with future measurements of the single top quark production in s and t channels [4].

In this Letter, we report the first simultaneous measurement of R and the top quark pair ($t\bar{t}$) production cross section $\sigma_{t\bar{t}}$. R was measured by the CDF and D0 collaborations [5, 6]. The simultaneous measurement of R and $\sigma_{t\bar{t}}$, in contrast to previous measurements [7, 8], allows one to extract $\sigma_{t\bar{t}}$ without assuming $\mathcal{B}(t \to Wb) = 1$, and to achieve a higher precision on both quantities by exploiting their different sensitivity to systematic uncertainties.

The current measurement is based on data collected with the D0 detector [9] between August 2002 and December 2005 at the Fermilab Tevatron $p\bar{p}$ collider at $\sqrt{s} = 1.96$ TeV, corresponding to an integrated luminosity of about 0.9 fb^{-1}, approximately four times larger than that of our previous measurement [6]. The analysis uses the top quark pair decay channel $t\bar{t} \to W^+qW^-\bar{q}$, with the subsequent decay of one W boson into two quarks, and the other one into an electron or muon and a neutrino. This is referred to as the lepton plus jets (ℓ+jets) channel. We select a data sample enriched in $t\bar{t}$ events by requiring ≥ 3 jets with transverse momentum $p_T > 20$ GeV and pseudorapidity $|\eta| < 2.5$ [10], one isolated electron with $p_T > 20$ GeV and $|\eta| < 1.1$ or muon with $p_T > 20$ GeV and $|\eta| < 2.0$, and missing transverse energy $\not\!\!E_T > 20$ GeV in the e+jets and $\not\!\!E_T > 25$ GeV in the μ+jets channel. Additionally, the leading jet p_T is required to exceed 40 GeV. Events containing a second isolated electron or muon with $p_T > 15$ GeV are rejected. The lepton isolation criteria are based on calorimeter and tracking information. Details of lepton, jets and $\not\!\!E_T$ identification are described elsewhere [10].

We identify b-jets using a neural-network tagging algorithm [11]. It combines variables that characterize the presence and properties of secondary vertices and tracks with high impact parameter inside the jet. In the simulation, we assign a probability for each jet to be b-tagged based on its flavor, p_T, and η. These probabilities are determined from data control samples, and can be combined to yield a probability for each $t\bar{t}$ event to have 0, 1, or ≥ 2 b-tagged jets [7].

We split the selected ℓ+jets sample into subsamples according to the lepton flavor (e or μ), jet multiplicity (3 or ≥ 4 jets) and number of identified b-jets (0, 1 or ≥ 2), thus obtaining 12 disjoint data sets. We fit simultaneously R and $\sigma_{t\bar{t}}$ to the observed number of 1 b tag and ≥ 2 b tag events, and, in 0 b tag events with ≥ 4 jets, to the shape of a discriminant $\mathcal{D}$ that exploits kinematic differences between the background and the $t\bar{t}$ signal and which is described in detail below. As the signal-to-background ratio is about five times smaller in events with 0 b tags and three jets we do not use a discriminant for that subsample.

The dominant background is the production of W bosons in association with heavy and light flavor jets (W+jets). Smaller contributions arise from Z+jets, diboson and single top quark production. Multijet events enter the selected sample if a jet is misidentified as an electron (e+jets), or a muon coming from either a semileptonic heavy quark decay or an in-flight pion or kaon decay in a light flavor jet appears isolated (μ+jets).

We model the signal and backgrounds other than multijet using a Monte Carlo (MC) simulation. The processes W+jets and Z+jets are generated with the ALPGEN 2.05 [12] leading-order event generator for the multiparton matrix element calculation and PYTHIA 6.323 [13] for subsequent parton showering and hadronization. Diboson samples are generated with PYTHIA and single top quark production is modeled using the SINGLETOP [14] generator. The $t\bar{t}$ signal is simulated with PYTHIA for a top quark mass of $m_{top} = 175$ GeV and includes three decay modes $t\bar{t} \to W^+bW^-\bar{b}$, $t\bar{t} \to W^+bW^-\bar{q}_l$ (or $t\bar{t} \to W^+q_lW^-\bar{b}$) and $t\bar{t} \to W^+q_lW^-\bar{q}_l$, where q_l denotes a light down-type (d or s) quark. These three decay modes are referred to as bb, bq_l and q_lq_l. The generated events are processed through the GEANT-based [15] simulation of the D0 detector. The same reconstruction

TABLE I: Sample composition for the measured $\sigma_{t\bar{t}}$ and $R = 1$. The uncertainties are statistical only.

$N_{\rm jets}$	sample	0 b tags	1 b tag	≥ 2 b tags
3	W+jets	1394.4 ± 48.4	102.5 ± 3.5	8.3 ± 0.3
	Multijet	287.4 ± 35.9	28.1 ± 3.5	3.3 ± 0.4
	Other	254.0 ± 1.9	29.4 ± 0.2	5.2 ± 0.4
	$t\bar{t}$	109.7 ± 0.4	143.3 ± 0.5	54.3 ± 0.2
	Total	2045.5 ± 60.3	303.3 ± 5.0	71.2 ± 0.5
	Observed	2050	294	76
4	W+jets	188.2 ± 15.0	17.3 ± 1.4	1.8 ± 0.1
	Multijet	66.9 ± 9.9	6.6 ± 1.0	0.8 ± 0.1
	Other	62.2 ± 0.9	8.0 ± 0.1	1.7 ± 0.0
	$t\bar{t}$	83.8 ± 0.3	126.4 ± 0.5	64.2 ± 0.2
	Total	401.1 ± 18.0	158.3 ± 1.8	69.5 ± 0.3
	Observed	389	179	58

algorithm as for data is used. Additional corrections [10] are applied to the reconstructed objects to improve the agreement between data and simulation.

The determination of the background composition starts with the evaluation of the multijet background for each jet multiplicity and lepton flavor before b-jet tagging by counting events in the corresponding control data samples and applying the matrix method [7]. We estimate the number of events with a lepton originating from a W or Z boson decay by subtracting the estimated multijet background from the observed event yield before b-tagging. We further subtract diboson, single top quark and Z+jets contributions, normalized to the next-to-leading order cross sections [16]. The remaining data events are assumed to come from $t\bar{t}$ and W+jets background. In the first step of the fitting procedure used to extract $\sigma_{t\bar{t}}$ and R, we assume the $t\bar{t}$ contribution predicted by the SM [17]. In every subsequent step, we iteratively re-determine the expected number of $t\bar{t}$ events and re-evaluate the W+jets background.

Since the probability to tag a $t\bar{t}$ event depends on the flavor of the jets, it depends on R. We estimate the acceptance and tagging probabilities for each of the three $t\bar{t}$ decay modes bb, bq_l and q_lq_l. Thus, the probability for a $t\bar{t}$ event to pass our selection criteria and to have n b-tagged jets is:

$$\begin{aligned} P^n_{total}(t\bar{t}) &= R^2 A(bb) P^n_t(bb) + 2R(1-R)A(bq_l)P^n_t(bq_l) \\ &+ (1-R)^2 A(q_lq_l)P^n_t(q_lq_l), \end{aligned}$$

where A (P^n_t) describes the acceptance (tagging probability) for each $t\bar{t}$ decay mode. Figure 1(a) shows P^n_t as a function of R for $t\bar{t}$ events with ≥ 4 jets and 0, 1 and ≥ 2 b tags. Table I presents the composition of the selected sample for the measured $\sigma_{t\bar{t}}$ and $R = 1$.

The topological discriminant $\mathcal{D}$ [10] exploits the kinematic differences between $t\bar{t}$ and W+jets events to achieve a better constraint on the number of $t\bar{t}$ events in the subsample with ≥ 4 jets and 0 b tags. We select variables well-described by the background model in samples of events with one or two jets that provide a good separation between signal and W+jets background. The optimal set of variables is chosen to minimize the expected statistical uncertainty on the fitted fraction of $t\bar{t}$ events. Due to the differences in acceptance and sample composition, the discriminants are constructed from different sets of variables in the e+jets and μ+jets channels. In the e+jets channel we use five variables: the leading jet p_T, the maximum $\Delta\mathcal{R}$ [10] between two of the four leading jets, $\mathcal{A}$, $\mathcal{C}_M$, and $\mathcal{D}_M$ [18]. In the μ+jets channel the discriminant is built from six variables: $\mathcal{A}$, $\mathcal{D}_M$, the scalar sum of the p_T of the four leading jets and the muon, the scalar sum of the p_T of the third and fourth jet in the event, the transverse mass of the vector sum of all jets, and the ratio of the mass of the three leading jets to the mass of the event, defined as the invariant mass of the vector sum of all four jets, the lepton from the W decay and the missing transverse energy coming from the neutrino. The sensitivity to soft radiation and to the underlying event is reduced by using only the four highest-p_T jets for the kinematic variables.

The discriminant function is built using simulated W+jets and $t\bar{t}$ events. We evaluate it for each physics process considered in the analysis and build corresponding template distributions consisting of ten bins. For $t\bar{t}$ we obtain a distribution for each of the three decay modes (bb, bq_l and q_lq_l). The shapes of the discriminant distributions for Z+jets, diboson and single top backgrounds are found to be similar to that of the W+jets events and we use the latter to model them. We use a sample of data events selected by requiring that the lepton fail the isolation criteria to obtain the discriminant shape for the multijet background.

We define a likelihood function as the product of Poisson probabilities over all 30 subsamples and bins of the discriminant, where in each subsample the expected number of events is estimated as a function of R and $\sigma_{t\bar{t}}$. We include 12 additional Poisson terms to constrain the multijet background prediction in each subsample. The systematic uncertainties are incorporated in the fit using nuisance parameters [19], each represented by a Gaussian term in the binned likelihood. In this approach, each source of systematic uncertainty is allowed to affect the central value of R and $\sigma_{t\bar{t}}$ during the likelihood maximization procedure, yielding a combined statistical and systematic uncertainty.

The result of the maximum likelihood fit is:

$$\begin{aligned} R &= 0.97^{+0.09}_{-0.08} \ \text{(stat+syst)} \ \text{and} \\ \sigma_{t\bar{t}} &= 8.18^{+0.90}_{-0.84} \ \text{(stat+syst)} \ \pm 0.50 \ \text{(lumi) pb} , \end{aligned}$$

for a top quark mass of 175 GeV. Figure 1(b,c) compares the distribution of the data to the sum of predicted background and measured $t\bar{t}$ signal for $R = 0.97$. We observe no significant dependence of R on m_{top} within ±10 GeV

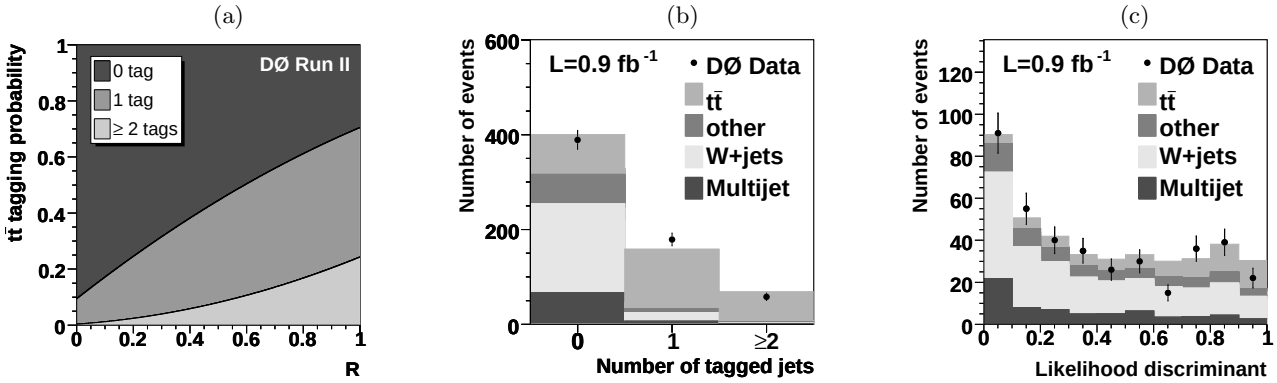

FIG. 1: (a) Fractions of events with 0, 1 and ≥ 2 b tags as a function of R for $t\bar{t}$ events with ≥ 4 jets; (b) predicted and observed number of events in the 0, 1 and ≥ 2 b tag samples for the measured R and $\sigma_{t\bar{t}}$ for events with ≥ 4 jets and (c) predicted and observed discriminant distribution in the 0 b tag sample with ≥ 4 jets.

around the assumed value while $\sigma_{t\bar{t}}$ changes by ∓ 0.09 pb per 1 GeV within the same range. We find a correlation between R and $\sigma_{t\bar{t}}$ of -58%. Table II summarizes the statistical and leading systematic uncertainties on R and $\sigma_{t\bar{t}}$ excluding the 6.1% uncertainty on the integrated luminosity [20]. The contribution of each individual source of uncertainty is estimated by fixing all but the corresponding Gaussian term in the fit. The statistical uncertainty is obtained from the fit with all Gaussian terms fixed.

The total uncertainty on R is about 9%, compared to 17% achieved in the previous measurement [6]. The largest uncertainty comes from the limited statistics. Since the b-tagging efficiency drives the distribution of the events among the 0, 1 and 2 b-tag subsamples and is strongly anti-correlated with R, the systematic uncertainty is dominated by the b-tagging efficiency estimation, responsible for $\sim$90% of the total systematic uncertainty.

The total uncertainty on $\sigma_{t\bar{t}}$, excluding luminosity, is $\sim$10.5%, representing a 30% improvement over the previous measurement [7] performed under the assumption of $R = 1$. In the latter, the primary 4.7% relative uncertainty comes from the b-tagging efficiency estimation while in the current measurement it is reduced to 1.2% because $\sigma_{t\bar{t}}$ is much less sensitive to the variations of the b-tagging efficiency than R, and the two-dimensional fit takes advantage of this feature.

We extract a limit on R and $|V_{tb}|$ following the Feldman-Cousins procedure [21]. We generate pseudo-experiments with all systematic uncertainties included for various input values of R ($R_{\rm true}$) and apply the likelihood-ratio ordering principle. We obtain $R > 0.88$ at 68% C.L. and $R > 0.79$ at 95% C.L., illustrated in Fig. 2. From R we determine the ratio of $|V_{tb}|^2$ to the off-diagonal matrix elements to be $\frac{|V_{tb}|^2}{|V_{ts}|^2+|V_{td}|^2} > 3.8$ at 95% C.L. Assuming a unitary CKM matrix with three fermion generations we derive $|V_{tb}| > 0.89$ at 95% C.L.

TABLE II: Summary of uncertainties on $\sigma_{t\bar{t}}$ and R.

Source	$\Delta\sigma_{t\bar{t}}$ (pb)	ΔR
Statistical	$+0.67\ -0.64$	$+0.067\ -0.065$
Lepton identification	$+0.32\ -0.27$	n/a
Jet energy scale	$+0.32\ -0.23$	n/a
W+jets background	$+0.21\ -0.23$	n/a
Multijet background	$+0.17\ -0.17$	$+0.016\ -0.016$
Signal modeling	$+0.12\ -0.25$	n/a
b-tagging efficiency	$+0.10\ -0.09$	$+0.059\ -0.047$
Other	$+0.24\ -0.13$	$+0.015\ -0.014$
Total uncertainty	$+0.90\ -0.84$	$+0.092\ -0.083$

In summary, we have performed a simultaneous measurement of the ratio of branching fractions R and $\sigma_{t\bar{t}}$ yielding the most precise measurements to date, $R = 0.97^{+0.09}_{-0.08}$ (stat+syst) and $\sigma_{t\bar{t}} = 8.18^{+0.90}_{-0.84}$ (stat+syst) $\pm$ 0.50 (lumi) pb, both in good agreement with the SM. This measurement of R will be a key ingredient in a future model-independent direct determination of the $|V_{tq}|$

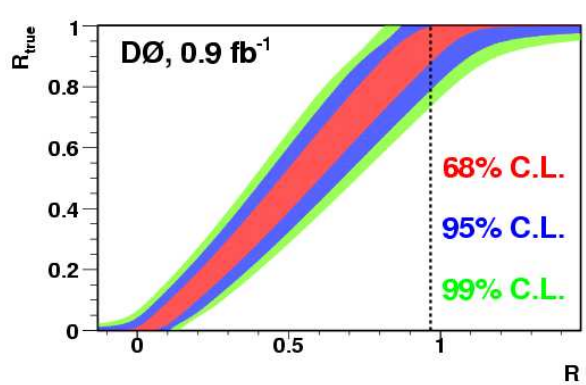

FIG. 2: The 68% (inner band), 95% (middle band) and 99% (outer band) C.L. bands for $R_{\rm true}$ as a function of R. The dotted black line indicates the measured value $R = 0.97$.

CKM matrix elements.

We thank the staffs at Fermilab and collaborating institutions, and acknowledge support from the DOE and NSF (USA); CEA and CNRS/IN2P3 (France); FASI, Rosatom and RFBR (Russia); CAPES, CNPq, FAPERJ, FAPESP and FUNDUNESP (Brazil); DAE and DST (India); Colciencias (Colombia); CONACyT (Mexico); KRF and KOSEF (Korea); CONICET and UBACyT (Argentina); FOM (The Netherlands); Science and Technology Facilities Council (United Kingdom); MSMT and GACR (Czech Republic); CRC Program, CFI, NSERC and WestGrid Project (Canada); BMBF and DFG (Germany); SFI (Ireland); The Swedish Research Council (Sweden); CAS and CNSF (China); Alexander von Humboldt Foundation; and the Marie Curie Program.

[a] Visitor from Augustana College, Sioux Falls, SD, USA.
[b] Visitor from The University of Liverpool, Liverpool, UK.
[c] Visitor from ICN-UNAM, Mexico City, Mexico.
[d] Visitor from II. Physikalisches Institut, Georg-August-University, Göttingen, Germany.
[e] Visitor from Helsinki Institute of Physics, Helsinki, Finland.
[†] Fermilab International Fellow.
[‡] Deceased.

[1] N. Cabbibo, Phys. Rev. Lett. **10**, 531 (1961); M. Kobayashi and T. Maskawa, Prog. Theor. Phys. **49**, 652 (1973).
[2] W.-M. Yao *et al.*, Journal of Physics G **33**, 1 (2006).
[3] D0 Collaboration, V. Abazov *et al.*, Phys. Rev. Lett. **98**, 181802 (2007).
[4] J. Alwall *et al.*, Eur. Phys. J. C **49**, 791 (2007).
[5] CDF Collaboration, T. Affolder *et al.*, Phys. Rev. Lett. **86**, 3233 (2001); CDF Collaboration, T. Affolder *et al.*, Phys. Rev. Lett. **95**, 102002 (2005).
[6] D0 Collaboration, V. Abazov *et al.*, Phys. Lett. B **639**, 616 (2006).
[7] D0 Collaboration, V. Abazov *et al.*, Phys. Rev. D **74**, 112004 (2006).
[8] CDF Collaboration, D. Acosta *et al.*, Phys. Rev. D **71**, 072005 (2005); CDF Collaboration, D. Abulencia *et al.*, Phys. Rev. Lett. **97**, 082004 (2006).
[9] D0 Collaboration, V. Abazov *et al.*, Nucl. Instrum. and Methods A **565**, 463 (2006).
[10] D0 Collaboration, V. Abazov *et al.*, Phys. Rev. D **76**, 092007 (2007).
[11] T. Scanlon, Ph.D. thesis, University of London, 2006.
[12] M.L. Mangano *et al.*, JHEP **07**, 001 (2003).
[13] T. Sjöstrand *et al.*, arXiv:hep-ph/0308153.
[14] E.E. Boos *et al.*, Phys. Atom. Nucl. **69**, 1317 (2006).
[15] R. Brun and F. Carminati, CERN Program Library Long Writeup W5013, 1993 (unpublished).
[16] Z. Sullivan, Phys. Rev. D **70**, 114012 (2004); J.M. Campbell and R.K. Ellis, Phys. Rev. D **60**, 113006 (1999).
[17] N. Kidonakis and R. Vogt, Phys. Rev. D **68**, 114014 (2003); M. Cacciari *et al.*, JHEP **404**, 68 (2004).
[18] The normalized momentum tensor, $\mathcal{M}$, is defined as $\mathcal{M}_{ij} = \frac{\Sigma_k p_i^k p_j^k}{\Sigma_k |\vec{p^k}|^2}$, where $\vec{p^k}$ is the momentum vector of a reconstructed object k, and i and j are Cartesian coordinates. Aplanarity $\mathcal{A}$, $\mathcal{C}_M$ and $\mathcal{D}_M$ are defined here as $\frac{3}{2}\lambda_3$, $3(\lambda_1\lambda_2 + \lambda_1\lambda_3 + \lambda_2\lambda_3)$ and $27\lambda_1\lambda_2\lambda_3$, respectively, where λ_1, λ_2 and λ_3 are the eigenvalues of $\mathcal{M}$.
[19] P. Sinervo, in *Proceedings of Statistical Methods in Particle Physics, Astrophysics, and Cosmology*, edited by L. Lyons, R. P. Mount, and R. Reitmeyer (SLAC, Stanford, 2003), p. 334.
[20] T. Andeen *et al.*, FERMILAB-TM-2365 (2007).
[21] G. Feldman and R. Cousins, Phys. Rev. D **57**, 3873 (1998).